

Demonstration of a Photonic Time-Multiplexed C-NOT Gate

Federico Pegoraro^{†,*}, Philip Held[†], Jonas Lammers[†], Benjamin Brecht, and Christine Silberhorn
*Paderborn University, Integrated Quantum Optics,
Institute of Photonic Quantum Systems (PhoQS) Warburger Str. 100, 33098, Paderborn, Germany*
(Dated: December 4, 2024)

The two-qubit controlled-not (C-NOT) gate is an essential component in the construction of a gate-based quantum computer. In fact, its operation, combined with single qubit rotations allows to realise any quantum circuit. Several strategies have been adopted in order to build quantum gates, among them the photonic one offers the dual advantage of excellent isolation from the external environment and ease of manipulation at the single qubit level. Here we adopt a scalable time-multiplexed approach in order to build a fully reconfigurable architecture capable of implementing a post-selected interferometric scheme that implements the C-NOT operation with a fidelity of $(93.8 \pm 1.4)\%$. We use our experimental platform to generate the four Bell states.

[†]: These authors contributed equally

The past decades witnessed a momentous race towards advances in quantum computation and communication science. At the foundation of any quantum computation scheme lays the quantum bit, or qubit: the fundamental information unit consisting of a quantum system of two levels corresponding to the logical $|0\rangle$ and $|1\rangle$ states. A variety of physical platforms have been employed in order to implement systems of one or multiple qubits: notable ones employing for instance spin of charged particles in semiconductors [28], atomic nuclei [13], trapped ions [6] and quantum dots [2], others exploiting vibrational energy levels in molecules [5], superconductive systems [11], or topological properties of two-dimensional systems [14]. An alternative paradigm is photonic quantum computing (PQC) [15, 16, 24]. In PQC photons are the carriers of quantum information, which is encoded in the degrees of freedom of the light quanta. This approach offers both excellent isolation between system and external environment and ease of manipulation of the single qubit states via linear optical elements. Complementary to information encoding is the need for operations capable of manipulating the information content of the quantum system of choice. For this reason it is necessary to be able to build logic quantum gates capable of acting on the state of one or many qubits. While single qubit gates can alter the state of individual information units, two- or more qubit operations influence the joint state of a system and introduce interaction between subsystems. Among the two-qubit gates the controlled-not (C-NOT) gate stands out for its capability of generating entanglement and is an essential component for the construction of arbitrary gate-based quantum circuits [1]. In spite of the inherently non-interactive nature of photons, the realization of a C-NOT gate based on linear optics is rendered possible by the adoption of ancillary modes and coincidence measurements in different interferometric schemes [24, 25]. Experimental implementations have demonstrated the C-

NOT adopting several encoding strategies involving a variety of light properties: many exploited path and polarization encoding both in bulk [22, 31] and integrated [9, 29, 30] optics, in other instances degrees of freedom as frequency [18, 19] or light orbital angular momentum [17] have been employed.

For scaling systems time-multiplexing (TM) has been explored in the recent years [21, 23, 26, 27] and has actually been harnessed to achieve quantum computation advantages in the scope of Gaussian boson sampling [20]. Yet, these systems are intrinsically not capable of achieving universal quantum computation, which requires C-NOT operations. Some work towards this goal has been carried out [12], but to this date a direct implementation of a fully TM C-NOT gate is missing.

Here we report on the first demonstration of a photonic C-NOT gate in a fully reconfigurable TM experimental platform. We show a TM interferometer capable of reproducing the scheme of [25] and we provide a complete characterization of its behavior. We use the described platform in order to reconstruct the C-NOT logical table of truth obtaining an excellent agreement with the expected one. Lastly, we show that the system can be programmed and used in order to generate the four Bell $|\Phi^\pm\rangle$ and $|\Psi^\pm\rangle$, thus proving the entangling power of our C-NOT gate as well as its suitability for the generation of powerful resource states for a wide range of applications such as quantum cryptography [10], quantum teleportation [4], dense coding [3], and violation of Bell inequalities [7].

I. RESULTS

A. Time-multiplexed interferometric scheme

TM is a scheme capable of realizing a PQC circuit in the time domain. In particular we seek to replicate the interferometer of Fig. 1a) using a TM architecture. This configuration initially proposed by Ralph *et al.* in [25]

* federico.pegoraro@uni-paderborn.de

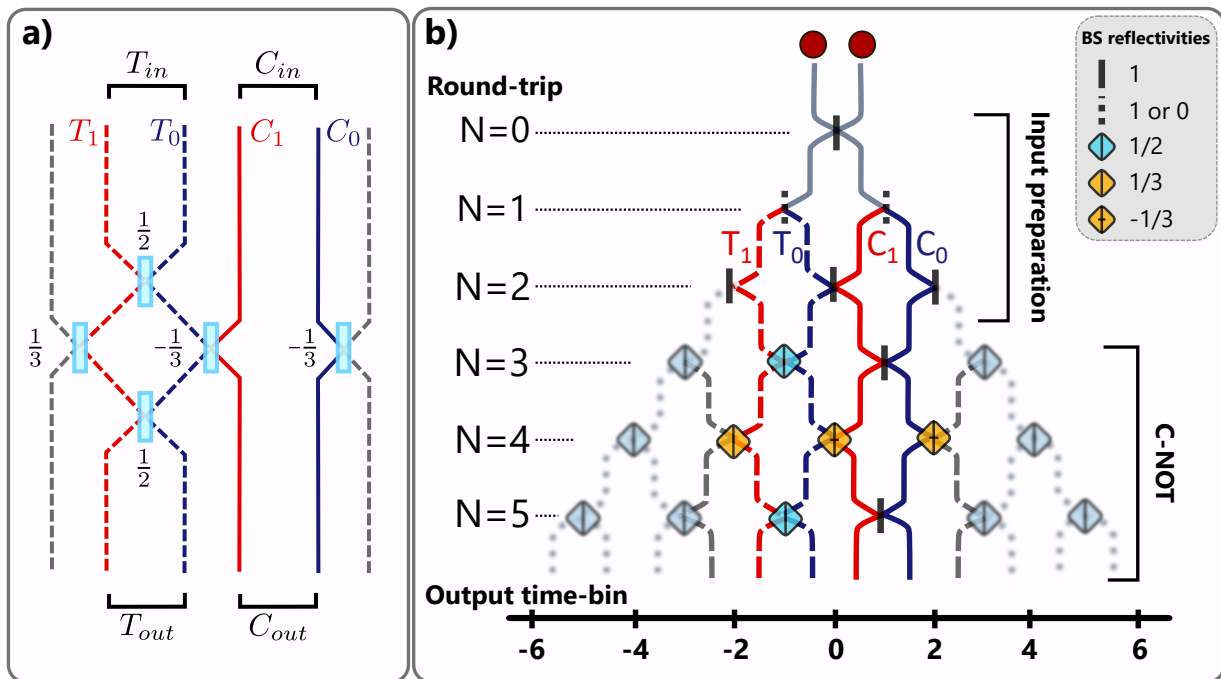


FIG. 1. **a)** Post-selected photonic C-NOT [25]. Two photons enter the 6×6 interferometer one in the control and the other in the target modes (C_{in} and T_{in}), the outermost modes (gray dashed lines) are ancillary channels required by the scheme; the C-NOT is successful upon detection of the two photons in the C_{out} and T_{out} modes. The absolute value of the fraction near each BS represents its reflectivity while the sign represents the propagation phase taken in reflection by a photon entering the BS from the left input. **b)** Schematic representation of the TM implementation of the C-NOT. Each row of the BS cascade represents a round-trip in the setup shown in Fig. 2. The action of each BS corresponds to a switch of an EOM acting on a time-bin; the switches are set to reproduce the C-NOT interferometer. The first two round-trips serve as input state preparation, while the remaining three perform the actual interferometer. The rightmost reflection of round-trip 3 can be reconfigured to a $\frac{1}{2}$ BS in order to reproduce the Hadamard-(C-NOT) circuit that generates the Bell states.

implements a photonic postselected C-NOT gate and requires two photons to encode the two-qubit state on which the gate is acting. The control and target qubits are initiated in the C_{in} and T_{in} input groups, respectively. They then propagate through a series of beamsplitters (BSs) with reflectivities of $\frac{1}{2}$ and $\pm\frac{1}{3}$, where the signs are linked to the the BS reflection phase setting (we are going comment on the phase settings in subsection IB). The gate is successful upon detection of a photon in the C_{out} and the other in T_{out} outputs. Translating this scheme to the TM paradigm requires to identify the interferometer inputs and outputs with a sequence of time-bins evolving into a looped structure. As shown in [8], any linear optical network implementing a unitary transformation can be decomposed into a structure featuring several layers of BSs and phase shifters. If we apply the same idea to a TM architecture we can interpret each evolutionary layer as a round-trip in the looped structure implementing the transformation. In Fig. 1b) we show a schematic depiction of this concept applied to the C-NOT interferometer. In this BS cascade each row represents a round-trip, while the position of each BS identifies a time-bin; the set of BSs within a round-trip is realized by the repeated action of a single component capable of addressing each time-bin

independently.

In practice we achieve this using an interferometric setup where delay lines, linear optical elements and fast, reconfigurable electro-optic modulators (EOMs) distribute and interfere the incoming light on a series of time-bins. Fig. 2 shows the structure of our TM setup, consisting of an unbalanced Mach-Zehnder interferometer with a feedback path. A light pulse impinges on a polarizing beamsplitter (PBS) that separates it into two pulses with H and V polarization. The two pulses will then travel to two single mode fibers of different lengths imparting a relative time delay of 170 ns between the two polarizations. Two electro-optical modulators (EOM₁ and EOM₂) are used to rotate the polarization of the two pulses by 90° and direct them to the feedback path located after a second PBS. This allows to deterministically in-couple light to the TM interferometer. This architecture is analogous to the ones seen in [21] and [23], where the scheme was used in the scope of discrete time quantum walks, whose evolution consists of a large network of beamsplitters (BSs) similar to the one of Fig. 1b), but with a reflectivity equal for all time-bins and round-trips. This was achieved employing a half-waveplate positioned in the feedback path. In this work we modify the structure by replacing the waveplate

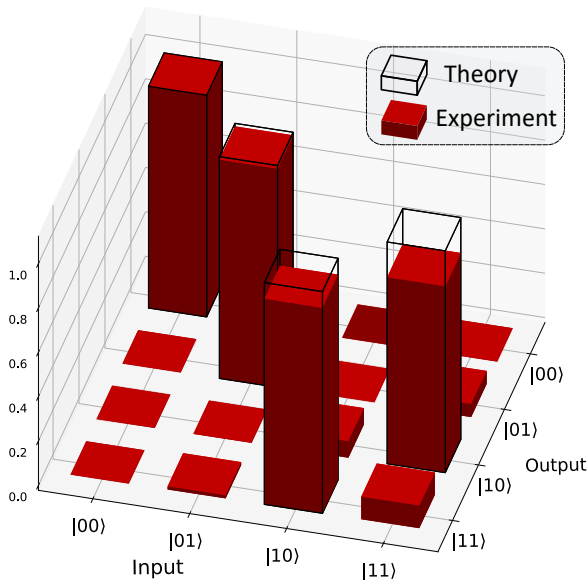


FIG. 3. Measured vs theoretical truth table for the TM C-NOT. From the measured coincidences we obtain operation probabilities of probability $P_{00} = 100.00\%$ and $P_{01} = 98.64\%$ for the $|00\rangle$ and $|01\rangle$ inputs, $P_{11} = 92.62\%$ and $P_{10} = 84.06\%$, for the $|10\rangle$ and $|11\rangle$ inputs. We estimate a gate operation fidelity of $(93.8 \pm 1.4)\%$.

in its classical counterpart, the state of the T-qubit is flipped if the C-qubit is in the logical $|1\rangle$ state, and stays unchanged when C is in the $|0\rangle$ state. In general, the action of the C-NOT is represented by a unitary transformation, which in the C-T joint basis $\{|00\rangle, |01\rangle, |10\rangle, |11\rangle\}$ takes the form:

$$U_{C-NOT} = \begin{pmatrix} 1 & 0 & 0 & 0 \\ 0 & 1 & 0 & 0 \\ 0 & 0 & 0 & 1 \\ 0 & 0 & 1 & 0 \end{pmatrix}. \quad (1)$$

The main challenge in the realization of a photonic C-NOT gate resides in the inherently non-interacting nature of photons. For this reason a photon based implementation of the gate require the addition of ancillary modes and post-selection on specific coincidence output patterns. The scheme of Fig. 1a) requires a combination of BSs with reflectivity of $\frac{1}{2}$, $\pm\frac{1}{3}$. For the BS operations we take into account unitaries with no imaginary phases where depending on the reflectivity setting $\pm R$ we have the transformation:

$$\hat{B}S_{\pm R} = \begin{pmatrix} \pm\sqrt{R} & \sqrt{1-R} \\ \sqrt{1-R} & \mp\sqrt{R} \end{pmatrix}, \quad (2)$$

Interaction between C and T subsystems is possible by means of HOM-like interference happening between two single photons in the C_1 an T input states. Bunching effects caused by this kind of interference produce a coincidence pattern that reproduce the outcome of the unitary

in Eq.1 upon detection of exactly one photon in the C and T outputs. In order to demonstrate the performance of our C-NOT gate, we require the preparation of suitable single photon input states.

As Fig. 1b) is showing, our experimental system is not only capable of implementing the C-NOT circuit but can also be configured to produce the C-T input state starting from the two photons coming from one generation event of our SPDC source. This is achieved using the fact that in our experimental scheme the two photons enter the network orthogonal polarizations, thus they are separated by the first PBS of the setup. Consequently, one of them will be delayed with respect to the other by the time $\Delta\tau$ introduced by the length difference of the two fiber loops. This corresponds to the zeroth round-trip of Fig. 1b), then the two photons can be directed to the desired control and target inputs by reflective or transmissive operations. In the TM scheme this is translated to the fact that EOM₃ shall act on the polarization state of two time-bins generated by the previous splitting either by flipping or keeping it untouched. The next round-trip serves the sole purpose of redirecting the photons to the inputs of the C-NOT, which is implemented in the following three round-trips by programming EOM₃ to reproduce the required $\frac{1}{2}$ and $\pm\frac{1}{3}$ BSs in the polarization space. This is rendered possible considering the fact that the combination of waveplates and EOM₃ allows us to perform the transformation over the incoming modes:

$$\hat{U}(\theta) = \begin{pmatrix} \sin(\theta) & \cos(\theta) \\ \cos(\theta) & -\sin(\theta) \end{pmatrix},$$

where $\theta \in [-35^\circ, 90^\circ]$, which allows to reproduce all the required BS settings (see Eq. 2), as well as fully transmissive and reflective operations that are modeled as the action of a BS with $R=0$ or $R=1$, respectively. This protocol allows to generate the four input states: $|00\rangle_{CT}, |01\rangle_{CT}, |10\rangle_{CT}, |11\rangle_{CT}$, let them evolve through the C-NOT interferometer and eventually detect the output coincidence patterns. Fig. 3 shows the comparison between the experimentally reconstructed and ideal C-NOT operation from which we obtain a gate fidelity of $(93.8 \pm 1.4)\%$. The obtained gate fidelity shows the excellent performance of our TM C-NOT gate and compares positively to other implementations both in bulk [22] and integrated optics [9].

The two main limiting factors bounding the operation fidelity are to be sought in the residual distinguishability of the two photons and spurious multi-photon generation events from the SPDC process. In the supplementary material we provide a detailed discussion of these effects. Our analysis shows that assuming an ideal gate operation the two aforementioned effects limit the operation fidelity to $\leq 95\%$, hence signifying an excellent gate operation.

A striking feature of the quantum version of the C-NOT gate is its ability to generate entanglement between control and target. This happens when the C-subsystem is initiated in a superposition state of the logical $|0\rangle$ and

$|1\rangle$. Specifically, the input states $|\pm\rangle_C|0\rangle_T$ and $|\pm\rangle_C|1\rangle_T$, where $|\pm\rangle = \frac{|0\rangle \pm |1\rangle}{\sqrt{2}}$, are transformed by the action of the C-NOT in the Bell states $|\Phi^\pm\rangle = \frac{|00\rangle_{CT} \pm |11\rangle_{CT}}{\sqrt{2}}$ and $|\Psi^\pm\rangle = \frac{|01\rangle_{CT} \pm |10\rangle_{CT}}{\sqrt{2}}$, respectively. We now proceed to show how our architecture can be reprogrammed to produce the Bells states $|\Phi^\pm\rangle$ and $|\Psi^\pm\rangle$. As stated above this can be achieved by putting the control qubit in a superposition state $|\pm\rangle$ before acting on the joint C-T state with the C-NOT. We accomplish this by replacing the rightmost reflection in the fourth row of Fig. 1b) with a BS with reflectivity of $\frac{1}{2}$. Here we must consider that, according to Eq. 2, a reflective operation takes the form of the $\hat{\sigma}_z$ Pauli operator. This means that the rightmost reflective switch of the last round-trip of Fig. 1b) will leave the $|0\rangle_C$ component of the state unchanged, while $|1\rangle_C$ is sent to $-|1\rangle_C$. The presence of this phase results in the following mapping for the Bell states:

$$\begin{aligned} |00\rangle_{CT} &\longrightarrow |\Phi^-\rangle_{CT} \\ |01\rangle_{CT} &\longrightarrow |\Psi^-\rangle_{CT} \\ |10\rangle_{CT} &\longrightarrow |\Phi^+\rangle_{CT} \\ |11\rangle_{CT} &\longrightarrow |\Psi^+\rangle_{CT} \end{aligned}$$

After the C-NOT we perform an additional round-trip where a series of reflections send each photon to an individual time-bin, as in this case the reflections affect both C and T qubits, they won't produce additional phase shifts in the joint output state. This last operation is carried out with the purpose of performing quantum state tomography in the detection scheme described at the end of subsection I A, for which the polarization state of each photon shall not be distributed over two different time-bins. For the reconstructed density operators we observe quantum fidelities with respect to the target states of $\mathcal{F}_{\Psi^-} = (76 \pm 7)\%$, $\mathcal{F}_{\Psi^+} = (84 \pm 12)\%$, $\mathcal{F}_{\Phi^-} = (85 \pm 6)\%$ and $\mathcal{F}_{\Phi^+} = (79 \pm 13)\%$. In Fig. 4b) we show the reconstructed density operator for the state $|\Phi^-\rangle$, while in Fig. 4a) we show the output patterns for each input C-T state recorded in the computational basis for which we observe an average fidelity of $(92.6 \pm 1.7)\%$.

II. DISCUSSION

In this work we reported on a TM scheme that exploits dynamical polarization operations to translate the photonic C-NOT interferometric scheme from a path to a temporal encoding with high fidelity. Moreover, the employed experimental platform grants us the ability to deterministically prepare different input control-target states, including superpositions at the single qubit level. This feature allows us to exploit our source efficiently by

using both photons from a single generation event, hence removing additional losses and phase instabilities deriving from heralding on consecutive generation instances.

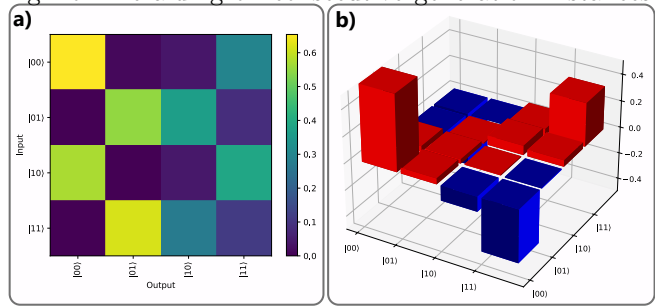


FIG. 4. **a)** Output patterns in the computational basis for the four Bell states. For the input states $|00\rangle$ and $|10\rangle$ we observe pronounced output contributions in the $|00\rangle$ and $|11\rangle$ outputs, corresponding to the structure of the $|\Phi^\pm\rangle$ Bell states. Conversely the $|01\rangle$ and $|11\rangle$ show significant contributions in the $|01\rangle$ and $|10\rangle$ outputs, reproducing the expectations for the $|\Psi^\pm\rangle$ states. The output pattern follows the predicted one with a fidelity of $(92.6 \pm 1.7)\%$. **b)** Reconstructed density operator for the state $|\Phi^-\rangle$ for which we observe a quantum fidelity $(85 \pm 6)\%$.

This ability is also crucial in order to generate entanglement between the two qubits and has allowed us to use our platform to produce the four Bell states. In this sense, we have shown that our TM scheme has the ability of performing both single- and two-qubit gates. Moreover, the inherently scalable nature of TM, allows us to envision an arbitrary large network based on the parallelization of TM-encoded photonic quantum gates. Hence, our result paves the way to the realization of more complex TM evolution networks featuring a multitude of input and output modes, with no significant limitation in the input states that can be launched in the the network.

III. ACKNOWLEDGEMENTS

The authors thank René Pollmann for the fruitful discussions. We acknowledge financial support by the European Commission through the Horizon Europe project EPIQUE (Grant No. 101135288).

IV. AUTHOR CONTRIBUTIONS

F.P., P.H., J.L. performed the experiments and analyzed the results. P.H. conceived the experimental scheme. F.P. performed the state reconstruction and led writing of the manuscript. P.H., J.L. assisted in writing the paper. C.S. and B.B. supervised the work. C.S. initiated the work. All authors discussed the results and commented on the manuscript.

-
- [1] Adriano Barenco, Charles H. Bennett, Richard Cleve, David P. DiVincenzo, Norman Margolus, Peter Shor, Tycho Sleator, John A. Smolin, and Harald Weinfurter. Elementary gates for quantum computation. *Physical Review A*, 52(5):3457–3467, November 1995.
- [2] Adriano Barenco, David Deutsch, Artur Ekert, and Richard Jozsa. Conditional quantum dynamics and logic gates. *Phys. Rev. Lett.*, 74:4083–4086, May 1995.
- [3] Charles H Bennett and Stephen J Wiesner. Communication via one-and two-particle operators on einstein-podolsky-rosen states. *Physical review letters*, 69(20):2881, 1992.
- [4] Charles H Bennett, Gilles Brassard, Claude Crépeau, Richard Jozsa, Asher Peres, and William K Wootters. Teleporting an unknown quantum state via dual classical and einstein-podolsky-rosen channels. *Physical review letters*, 70(13):1895, 1993.
- [5] Eduardo Berrios, Martin Gruebele, Dmytro Shyshlov, Lei Wang, and Dmitri Babikov. High fidelity quantum gates with vibrational qubits. *The Journal of Physical Chemistry A*, 116(46):11347–11354, 2012.
- [6] J. I. Cirac and P. Zoller. Quantum computations with cold trapped ions. *Phys. Rev. Lett.*, 74:4091–4094, May 1995.
- [7] John F Clauser, Michael A Horne, Abner Shimony, and Richard A Holt. Proposed experiment to test local hidden-variable theories. *Physical review letters*, 23(15):880, 1969.
- [8] William R Clements, Peter C Humphreys, Benjamin J Metcalf, W Steven Kolthammer, and Ian A Walmsley. Optimal design for universal multiport interferometers. *Optica*, 3(12):1460–1465, 2016.
- [9] Andrea Crespi, Roberta Ramponi, Roberto Osellame, Linda Sansoni, Irene Bongioanni, Fabio Sciarrino, Giuseppe Vallone, and Paolo Mataloni. Integrated photonic quantum gates for polarization qubits. *Nature communications*, 2(1):566, 2011.
- [10] Artur K Ekert. Quantum cryptography based on bell’s theorem. *Physical review letters*, 67(6):661, 1991.
- [11] He-Liang Huang, Dachao Wu, Daojin Fan, and Xiaobo Zhu. Superconducting quantum computing: a review. *Science China Information Sciences*, 63(8), July 2020.
- [12] Peter C Humphreys, Benjamin J Metcalf, Justin B Spring, Merritt Moore, Xian-Min Jin, Marco Barbieri, W Steven Kolthammer, and Ian A Walmsley. Linear optical quantum computing in a single spatial mode. *Physical review letters*, 111(15):150501, 2013.
- [13] J. A. Jones and M. Mosca. Implementation of a quantum algorithm on a nuclear magnetic resonance quantum computer. *The Journal of Chemical Physics*, 109(5):1648–1653, 08 1998.
- [14] A.Yu. Kitaev. Fault-tolerant quantum computation by anyons. *Annals of Physics*, 303(1):2–30, January 2003.
- [15] Emanuel Knill, Raymond Laflamme, and Gerald J Milburn. A scheme for efficient quantum computation with linear optics. *nature*, 409(6816):46–52, 2001.
- [16] Pieter Kok, William J Munro, Kae Nemoto, Timothy C Ralph, Jonathan P Dowling, and Gerard J Milburn. Linear optical quantum computing with photonic qubits. *Reviews of modern physics*, 79(1):135–174, 2007.
- [17] JH Lopes, WC Soares, Bertúlio de Lima Bernardo, DP Caetano, and Askery Canabarro. Linear optical cnot gate with orbital angular momentum and polarization. *Quantum information processing*, 18:1–10, 2019.
- [18] Hsuan-Hao Lu, Joseph M Lukens, Brian P Williams, Poolad Imany, Nicholas A Peters, Andrew M Weiner, and Pavel Lougovski. A controlled-not gate for frequency-bin qubits. *npj Quantum Information*, 5(1):24, 2019.
- [19] Hsuan-Hao Lu, Joseph M Lukens, Muneer Alshowkan, Brian T Kirby, and Nicholas A Peters. Building a controlled-not gate between polarization and frequency. *Optica Quantum*, 2(4):282–287, 2024.
- [20] Lars S Madsen, Fabian Laudenbach, Mohsen Falamarzi Askarani, Fabien Rortais, Trevor Vincent, Jacob FF Bulmer, Filippo M Miatto, Leonhard Neuhaus, Lukas G Helt, Matthew J Collins, et al. Quantum computational advantage with a programmable photonic processor. *Nature*, 606(7912):75–81, 2022.
- [21] Thomas Nitsche, Fabian Elster, Jaroslav Novotný, Aurél Gábris, Igor Jex, Sonja Barkhofen, and Christine Silberhorn. Quantum walks with dynamical control: graph engineering, initial state preparation and state transfer. *New Journal of Physics*, 18(6):063017, 2016.
- [22] Jeremy L O’Brien, Geoffrey J Pryde, Andrew G White, Timothy C Ralph, and David Branning. Demonstration of an all-optical quantum controlled-not gate. *Nature*, 426(6964):264–267, 2003.
- [23] Federico Pegoraro, Philip Held, Sonja Barkhofen, Benjamin Brecht, and Christine Silberhorn. Dynamic conditioning of two particle discrete-time quantum walks. *Physica Scripta*, 98(3):034005, 2023.
- [24] T. B. Pittman, B. C. Jacobs, and J. D. Franson. Probabilistic quantum logic operations using polarizing beam splitters. *Phys. Rev. A*, 64:062311, Nov 2001.
- [25] Timothy C Ralph, Nathan K Langford, TB Bell, and AG White. Linear optical controlled-not gate in the coincidence basis. *Physical Review A*, 65(6):062324, 2002.
- [26] A Schreiber, KN Cassemiro, V Potoček, A Gábris, I Jex, and Ch Silberhorn. Decoherence and disorder in quantum walks: from ballistic spread to localization. *Physical review letters*, 106(18):180403, 2011.
- [27] Andreas Schreiber, Katuscia N Cassemiro, Václav Potoček, Aurél Gábris, Peter James Mosley, Erika Andersson, Igor Jex, and Ch Silberhorn. Photons walking the line: a quantum walk with adjustable coin operations. *Physical review letters*, 104(5):050502, 2010.
- [28] Lieven M. K. Vandersypen and Mark A. Eriksson. Quantum computing with semiconductor spins. *Physics Today*, 72(8):38–45, 08 2019.
- [29] Jonas Zeuner, Aditya N Sharma, Max Tillmann, René Heilmann, Markus Gräfe, Amir Moqanaki, Alexander Szameit, and Philip Walther. Integrated-optics heralded controlled-not gate for polarization-encoded qubits. *npj Quantum Information*, 4(1):13, 2018.
- [30] Qian Zhang, Meng Li, Yang Chen, Xifeng Ren, Roberto Osellame, Qihuang Gong, and Yan Li. Femtosecond laser direct writing of an integrated path-encoded cnot quantum gate. *Optical Materials Express*, 9(5):2318–2326, 2019.
- [31] Zhi Zhao, An-Ning Zhang, Yu-Ao Chen, Han Zhang, Jiang-Feng Du, Tao Yang, and Jian-Wei Pan. Experi-

Supplemental information: Demonstration of a Photonic Time-Multiplexed C-NOT Gate

V. MODELLING OF BEAMSPLITTERS AND EFFECT OF PHASE SHIFTS

The BS constitutes the core element of many linear optical networks. Its action on the state of an incoming photon is parametrized by the unitary operation:

$$\hat{U}(R, T, \phi_R, \phi_T) = \begin{pmatrix} \sqrt{R}e^{i\phi_R} & \sqrt{T}e^{-i\phi_T} \\ \sqrt{T}e^{i\phi_T} & -\sqrt{R}e^{-i\phi_R} \end{pmatrix}, \quad (1)$$

where R and T can be physically understood as the BS reflectivity and transmissivity, which in the lossless case satisfy the energy conservation condition $R+T = 1$. The two remaining parameters ϕ_R and ϕ_T represent the phases imposed on transmitted and reflected light, respectively. In this work we consider BS operations where $\phi_T = 0$ and reflection phases ϕ_R of either 0 or π . Taking into account the relation between transmission and reflection parameters, the class of BS unitaries that we want to implement reduce to:

$$\hat{U}_{\pm R} = \begin{pmatrix} \pm\sqrt{R} & \sqrt{1-R} \\ \sqrt{1-R} & \mp\sqrt{R} \end{pmatrix}. \quad (2)$$

We restrict to these two particular case because splitting operations we implement involve the polarization degree of freedom light and we can reconstitute the operations of Eq. 2 to the action of a half-waveplate with its fast axis oriented at an angle $\theta = \frac{1}{2}\cos^{-1}(\sqrt{R})$.

VI. TWO-QUBIT TOMOGRAPHY SETUP

Photons coming from the TM setup travel to a 50:50 BS, this allows to probabilistically separate time-bins carrying a two-qubit state encoded in the joint polarization of the two photons. After they are split, the both photons pass through a combination of a half- and quarter-wave plates installed into motorized rotation mounts that we use to set the wave plate axes to implement projections on the Pauli bases according to the angle settings:

	HWP	QWP
σ_x	22.5°	0°
σ_y	45°	-45°
σ_z	0°	0°

After the two waveplates a PBS separates H and V polarized light and direct it to two SNSPDs. Such a combination of wave plate and PBSs allow to reconstruct the polarization of a single qubit, hence by employing two of them we can retrieve the joint polarization state of the two photons. We use this scheme in order to reconstruct the density operators of the Bell states generated combining C-NOT and Hadamard gate.

VII. GATE FIDELITY BOUNDS

In the following we expand on effects of experimental imperfections outside time multiplexed C-NOT circuit limiting the maximum fidelity for the reconstructed gate logic table. As stated in the main text, we employ a Type-II SPDC process pumped with a single pulse to generate our control-target (c-t) pair consisting of a two mode squeezed state. Using the scheme discussed in the Results section, we can route the signal and idler photons to the desired c-t input combination. As a first consideration, we must take into account that the spectral properties of both signal and idler fields are not completely identical. Hence, the two will not be perfectly indistinguishable. We quantified the signal-idler

degree of indistinguishability using HOM interference obtaining a visibility $V = (98 \pm 1)\%$. We start by considering the expression of the two-mode squeezed state in terms of photon number states, which can be written as:

$$|\Psi\rangle = \sqrt{1 - |\lambda|^2} \sum_{n=0}^{\infty} \lambda^n \left(\sqrt{V} \hat{a}_c^\dagger + \sqrt{1 - V} \hat{b}_c^\dagger \right)^n \left(\hat{a}_t^\dagger \right)^n |\emptyset\rangle, \quad (3)$$

where $|\emptyset\rangle$ is the vacuum state, \hat{a}^\dagger and \hat{b}^\dagger are the creation operators associated to indistinguishable and distinguishable photons, V is the degree of indistinguishability between signal and idler and λ regulates the relative weight between contributions corresponding to different number of photons present in the signal-idler pair. The absolute value of λ can be tuned by setting the power of the pump field, as we want to use a photon pair to encode the input state of the gate, we use this dependence to limit the probability of producing more than two photons per generation. By imposing a mean photon number of 0.01 photons per generation we expect the probability of a two photon event to be $P(2) \approx 98\%$ of all successful generations instances, while the probability for a four photons event will be $P(4) \approx 2\%$ and higher contributions can be neglected.

Considering the transmission, round-trip and detection efficiencies of our setup, the probability that a two-photon state is detected after the 6 round-trips required to implement the C-NOT gate is $\approx 0.33\%$. Of all the detected two photon events, we expect a fraction V to come from indistinguishable particles. If we assume a perfect C-NOT interferometer, all the indistinguishable events will give correct contributions in the output truth table, while the distinguishable can result incorrect outcomes depending on the c input state. The C-NOT circuit has a success probability of $\frac{1}{9}$, thus two indistinguishable photons have a probability $P(2)P_D(2)V\frac{1}{9} \approx 0.036\%$ of being measured in the correct output mode combination. On the other hand, distinguishable contributions have a probability of $\approx 0.00054\%$ to give valid pattern to the C-NOT truth table when c is initiated in the $|0\rangle$ state. Conversely, if the c qubit starts in the $|1\rangle$ state, then pairs of distinguishable photons can contribute to both the desired output pattern with a probability of $\approx 0.00054\%$, as well as giving wrong output patterns with a probability of $\approx 0.0011\%$.

In addition to errors coming from non-perfect indistinguishability in the two-photon case, we simulate the effect of four-photon states coming from the source and propagating in the interferometer. We include this contribution in our analysis because our detectors cannot resolve the number of photons that triggered a detection instance, thus there is the possibility of reading out a c - t coincidence event coming from a four-photon input without being able to distinguish it from a true two-photon contribution. In this case we restrict the analysis only to the indistinguishable case as the probability of a contribution from a four-photon event with distinguishable photons is negligible. Finally we take into account that, due to imperfections in the detection part of our setup, we have a polarization resolution error resulting in a 1% probability for a qubit in the $|1\rangle$ state to be wrongly detected as a $|0\rangle$.

Considering all the above factors, for each input c - t combination we can calculate the probabilities for correct or wrong outcomes both for two- and four-photons generation events in the distinguishable (dist) and indistinguishable (indis), which we list in Tab. 1.

	$(c=0, t=0)$	$(c=0, t=1)$	$(c=1, t=0)$	$(c=1, t=1)$
Correct				
$P(n=2, \text{indis})$	0.036%	0.036%	0.036%	0.036%
Error				
$P(n=2, \text{indis})$	0%	0.00036%	0.00072%	0%
Correct				
$P(n=2, \text{dis})$	0.0017%	0.0010%	0.00061%	0.0017%
Error				
$P(n=2, \text{dis})$	0%	0.000010%	0.0012%	0.0011%
Correct				
$P(n=4, \text{indis})$	0.0019%	0.0019%	0.0015%	0.0015%
Error				
$P(n=4, \text{indis})$	0.00094%	0.00095%	0.0011%	0.0010%
P_{Success}	0.039%	0.038%	0.037%	0.039%
P_{Error}	0.00094%	0.0013%	0.0029%	0.0021%
P_{C-NOT}	98%	97%	93%	95%

TABLE I. Probabilities for different input patterns depending on photon number and indistinguishability. For all cases we consider the probability for a given contribution of the PDC to give a correct outcome or an error. The overall probability for success and error are obtained by summing the individual contributions. P_{C-NOT} is the probability that the input state is transformed into the expected logical output, assuming an ideal C-NOT gate.

The overall probability for correct or wrong outcomes is then obtained by summing the individual contributions,

while the probability of observing the expected C-NOT outcome given an imperfect input state is given by

$$P_{C-NOT} = \frac{P(\text{Success})}{P(\text{Success}) + P(\text{Error})}. \quad (4)$$

As it emerges from this analysis, the two c_0 inputs feature working probabilities of 97% and 98%, whereas in the c_1 cases the working probabilities are bound to 93% and 95%, the reduced probability for latter case has to be ascribed to the interplay between indistinguishability and higher photon number contributions. By averaging on the estimated working probabilities we can give an upper bound for the fidelity of the C-NOT operation for which we obtain a value of $F_{max} = 95.5\%$.